

FLUID-STRUCTURE INTERACTION:
Applications in the context of a flow in arterial
medium

JAUBERT D. , MOREAU V.

04.02.97 updated 16.07.1997

U.M.R. 5502 IMFT-CNRS-UPS
U.F.R. MIG Université Paul Sabatier
Bat. 1R2 118 route de Narbonne
31062 TOULOUSE
C.R.S. 4
Via Nazario Sauro, 10
09123 Cagliari, Italie

Abstract

The purpose of this study is to describe fluid-wall interactions in the aortic arch. We analyse a method which allows coupling between fluid equations (Navier-Stokes) and structure.

keywords: Fluid-structure interaction, aorta, elastic, deformation.

Nomenclature

E	Young coefficient
E_L	Elastance
h	Wall thickness
$R(z,t)$	Arterial Radius
t	time
u	longitudinal velocity
w	radial velocity
C	compliance
α	Womersley coefficient
η	parietal radial displacement
ξ	parietal longitudinal displacement
ν	Poisson coefficient
μ	blood viscosity
ρ	blood volumetric mass
ρ_w	arterial wall volumetric mass
τ	parietal constraint

1 INTRODUCTION

1.1 Fluid-structure Interaction

Since many years, the study of mechanic behavior has been divided in two sub-domains: fluid mechanics and structure mechanics. However these domains interact, specially for the treatment of the limit conditions. This kind of studies have several applications: aeronautic (flow around a wing profile), biomechanics (evolution of a red blood cell in a capillary network). The individual analysis of these sub-domains leads to approximations more or less appropriate on the fluid-structure interaction.

The numerical simulation of a fluid flow requires constraints proper to the resolution method (CFL, order or choice for the discretization schemes).

For these reasons, the problem of the connectivity of these two sub-domains across the interface arises. From this point of view, two conceptions neatly appear: an approach by un-coupling fluid and structure problems with a special treatment at the interface and a unitary approach for the management of these two sub-domains.

The second type of resolution is unfortunately expensive in computational time and in memory storage.

The first approach presents the advantage of minimizing the efforts, treating the individual problems and then concentrating on the interface treatment. A few questions arise in this treatment:

- first, it is important to understand if the insertion of a new formalism in the treatment of the limit conditions will not modify the global stability of the system even if the two sub-domains are stabilized (Maday);
- second, the impossibility of an implicit treatment in the temporal evolution which is common to both the sub-domains. This constraint leads to different treatments in the algorithm for the fluid structure passage. Usually the implemented algorithms choose either to treat the flow on the configuration at the previous time or predict the new position of the structure (Charbel Farhat). Differences in the nature of the sub-domains lead to differences in the mesh structure. For this reason, the passage from one domain to the other can lead to imprecisions and instabilities. Then, we have probably to recourse to a mortar type method to join together functions defined on the two meshes (Maday, Faker).
- Finally, a supplementary difficulty consists in the fact that the structure equations are formulated in Lagrangian coordinates while the fluid equations are typically written in Eulerian coordinates. A solution to this kind of problems is to use an “Arbitrary Lagrangian Eulerian (ALE)” method for which the frame of reference is neither linked to the fluid nor to the structure (Hirsch).

2 Study specific to the arterial medium

2.1 Introduction

For several reasons fluid-structure coupling is the main problem when dealing with the arterial medium. The pulsatile character of the blood circulation implies a strong interaction between the blood and the vascular wall. This characteristic is important to have continuity in the blood irrigation (oxygen and energy feeding) of the different organs of the human body. In fact, the heart contraction during a cardiac circle is divided in two steps, a systolic (blood ejection) and a diastolic one (ventricles fill-up). During the systole, the vascular wall deformation accumulates, as elastic energy, part of the mechanical energy that will be given back in the diastolic phase (Windkessel model). This mechanism assures approximately constant velocity and pressure at the capillary level.

This study is also linked to the importance of the characterization of the parietal constraints inside the pulsed boundary layer, in order to understand tissue tearing phenomenon or atherogenesis which can lead to arteriopathy such as aneurysm or stenosis formation (Caro & al. 71).

Modeling of blood flow in the arterial network is not easy because of the characteristics both of the blood and the vascular wall. Blood is composed of corpuscles and platelets in suspension in the plasma. The fluid viscosity is function of the flow shear rate. In addition, many parameters, such as the hematocrite (ratio of blood cells volume and total blood volume), have a role in the rheological analysis of the constitutive fluid. The vascular wall possesses a complex visco-elastic rheologic behavior with hysteresis. To make the problem affordable, we impose a certain number of restrictions according to the specific media on which we intend to work.

Let us consider the limits of the modeling concerning the characterization of the blood and the vascular wall. In the big arteries we can approximate blood as a Newtonian fluid, due to the importance of the Reynolds and Womersley numbers. Yet, the more the arterial diameter diminishes, the more the plasma layer diminishes and the flow velocity decreases. As a consequence, the fluid characteristics are intimately linked to the red cells behavior and principally to their de-formability. The blood is then strongly non-Newtonian and under diphasic evolutions governed by separation of phase effects (Fharaeus and Fharaeus-Lindqvist effects).

At the arterial walls, the visco-elastic character is preponderant in the big arteries and negligible in the capillary network.

A brief review of the analysis conducted for this type of flow in the last twenty years will be given in the following.

2.2 Analysis of the other approaches

The description of a pulsed flow in arterial medium is based on the continuum mechanics principles. The rheologic specification of the blood and the arterial wall determines the dynamics of the fluid and the wall. The fluid-structure

interaction is simulated by a coupling of the limit conditions. Even with simplifying hypothesis on the rheologic specifications, such as Newtonian behavior for the fluid and purely elastic one for the wall, we are led to a 3D study of the fluid (Navier-Stokes) and of the vascular wall (Navier). Some simplifications are then necessary to obtain theoretically and numerically satisfactory solutions. As the fluid flows along the vessel, it forces the arterial wall to move in the radial and longitudinal directions. If the vessel behaves in a passive way, its displacement is caused by the modifications of the trans-wall pressure, the visco-elastic properties of the wall and the inertial forces due to the effective mass of the vascular wall (Pedley 1980). Supposing negligible the inertia of the vascular wall, as well as that of the fluid and wall viscosity, the wall displacement is only given by the equilibrium between the pressure waves and the elastic forces. This can be expressed as a pressure-section relation:

$$A = A(P, t).$$

Many efforts have been done to determine this relation. There are works based on the approximation of the wave celerity (Anliker 1980) or on an expression of the arterial compliance (Stergipoulos & al 1992, Tardy 1992). About this approximation of the parietal movement, different fluid models have been developed.

Initially, they were concentrated on the linearized Navier-Stokes equations and in the frame of small elastic deformations (Womersley 1957b, Atabek 1968). Unfortunately these hypothesis are irrelevant in the velocity profile description, specially in big arteries. This fact has been noticed by Ling et Atabek (1972), who have developed a non-linear model called "local flow theory". This theory only permits to obtain local information on the velocity profile and it proscribes a resolution along an artery. By a succession of integration of this system we can remedy the restriction of the local model to obtain a global resolution. In fact, this kind of resolution is intimately linked to an approximation of the parietal constraint evaluation (Lambossy 1952, Zielke 1968, Trikha 1975, Kufahl 1985, Khalid-Naciri 1988, Zagzoule 1991, Mederic 1991, Yama & al. 1995, Lagrée & Rossi 1996). Another approach for the resolution of this kind of problem has been proposed. It consists in using an iterative process initialized by the two precedent models (Buthaud 1976, Atabek 1980, Doufoulkar 1995).

Many other studies concern the parietal movement influence and its role in the hemodynamic characteristics. They cast a doubt on the passive behavior of the arterial wall, which was an hypothesis of many models: from a dynamical (Dutta 1989, Klanchar 1990), a visco-elastic (Flaud 1979) and finally a geometrical point of view (Belardinelli 1995).

Recently, numerous studies have been conducted on the fluid-structure interaction, more formally and realistically on the influence of the active behavior of the wall on the hemodynamics (Perkthold 1995, Perkthold 1994, Ma & al 1992, Reuderink 1991). In the same spirit, using the blood incompressibility approximation, Magnaudet & al, Rivero 1995, Blanco 1995 have proposed to solve the deformation of the fluid-structure interface through the resolution of

the Stokes equation (projection method) for a flow around a bubble. We should add to this fluid-structure interaction problem, the importance of the distal limit conditions in order to closely characterize the down flow arterial network. This treatment is by its own a complex fluid structure interface, which is specific to each region of the human body that we want to analyze: bifurcations (Reuderink 1991), peristaltic contraction (Laurens 1995), stenosis (Porenta & al. 1989).

3 Resolution in the aortic arch

During this intensive research period we have tried to analyze the fluid-structure interaction in an elastic curved tube (representing the aortic arch) and we have decided to separate the fluid and structure problems from one another.

3.1 Fluid resolution

The fluid flow resolution is sought in the frame of the Navier-Stokes equation for an incompressible medium. For this, we have used the N3S software, provided by Simulog. This software solves the Navier-Stokes equations taking into account the deformation of the computational domain during the simulation. The algorithm is based on an Arbitrary Lagrangian Eulerian (ALE) method, consisting of the computation, at every time step, of a domain velocity which conforms to the boundary movement (through the limit conditions satisfied at the boundary), while it could be quite arbitrary inside the domain, where the only constraint is to keep a good quality mesh. This velocity is then used both in the transport term of the Navier-Stokes equations and to construct the next mesh.

3.2 Wall displacement

In a first time, we have considered a parietal displacement governed by a linear pressure-section law related to a coefficient, elastance (E_L), which depends on the material. We have used the following relation:

$$R^2 = R_0^2 \left(1 + \frac{P - P_0}{E_L} \right), \quad (1)$$

with R_0 the artery radius at the reference pressure P_0 (that corresponds to the external pressure). The aortic evolution is principally led by the trans-wall pressure.

Yet, as we have previously mentioned, the vascular wall structure is anisotropic and could be described in the frame of thin shells, through the Navier equations written as:

$$\rho_w h \frac{\partial^2 \eta}{\partial t^2} = P - P_0 - 2\mu \frac{\partial u}{\partial r} - \frac{Eh}{1 - \nu^2} \left(\frac{\nu}{R} \frac{\partial \xi}{\partial z} + \frac{\eta}{R^2} \right)$$

$$\rho_w h \frac{\partial^2 \xi}{\partial t^2} = -\mu \left(\frac{\partial w}{\partial r} + \frac{\partial u}{\partial z} \right) + \frac{Eh}{1-\nu^2} \left(\frac{\nu}{R} \frac{\partial \eta}{\partial z} + \frac{\partial \xi^2}{\partial z^2} \right).$$

The variables η and ξ represent the radial and longitudinal vessel evolution in the local base. If we consider as negligible the viscous effects and the longitudinal vascular wall displacement, we can write the previous equations in the following form:

$$\rho_w h \frac{\partial^2 \eta}{\partial t^2} = P - P_0 - \frac{Eh}{1-\nu^2} \left(\frac{\eta}{R^2} \right). \quad (2)$$

4 APPLICATIONS

4.1 Boundary Conditions

We choose to put non-homogeneous Dirichlet limit conditions at the aorta inlet. Only the amplitude, not the spatial profile, is function of time. At the outlet we give the classical Neumann condition:

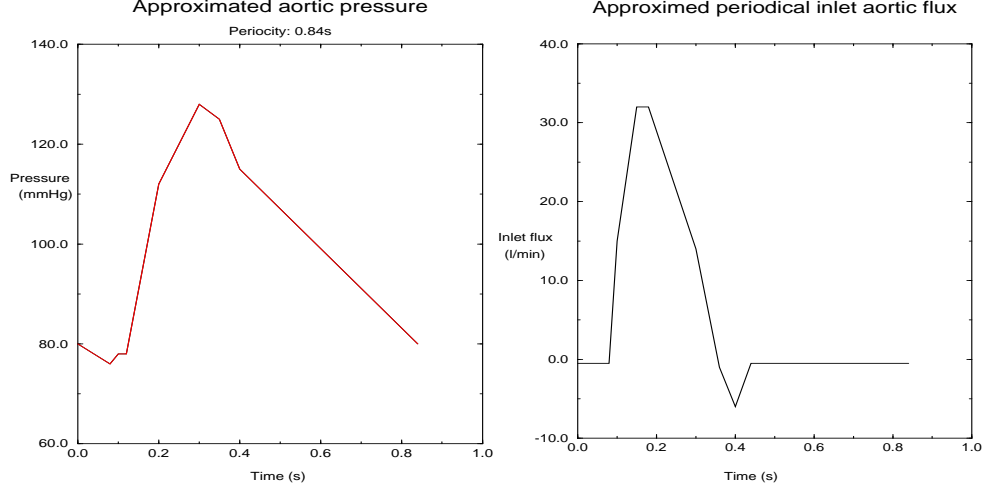
$$(-P.I + \nu \nabla u) \cdot n = \bar{P} \quad (3)$$

where I is the identity matrix and n the outward normal.

On the moving boundaries, we fix the velocity of the fluid equal to the velocity of the elastic structure not to have either cavitation or permeability. Being the fluid incompressible, the pressure is defined up to an additive constant which is enforced by setting the mean pressure \bar{P} at the outlet. In incompressible fluids, a problem is that pressure tends to lose its physical meaning, being considered either as a Lagrange multiplier or as the variable used to build the projection operator on the divergence free subspace. Unfortunately, while the resolution of the fluid velocity is indifferent to the pressure interpretation, it is definitively not the case for the resolution of the structural part, where the reference level of pressure and more generally its temporal evolution is essential. To treat this problem, we decided to re-normalize the pressure coming from the fluid resolution by a quantity only dependent on the temporal variable and satisfying the inlet pressure condition, given as a temporal variation on the mean value (since our physiological data are more precise at the inlet of the aorta). A validating criteria for the system evolution would be represented by a good behavior of the pressure at the outlet of the domain. This procedure does not seem completely satisfactory, however it was selected by the authors as the simplest choice available.

4.2 Mesh

The geometry construction and the generation of the initial mesh were made using the SIMAIL software from Simulog. Figure (1) shows the geometric structure of our domain and the mesh of reference we used for most of our runs.



4.3 Overview of the numerical algorithm

We suppose that the quantities: $\eta^{n-1}, \eta^n, P^n, u^n, x^n, \Gamma^n$, are known.

We recall that η is the displacement of the moving elastic wall. Γ is the moving fluid boundary, P the pressure, u the velocity of the fluid, x the position of the mesh and the subscript n indicates the value at time $t = t^n = t_0 + n.\Delta t$. Without loss of generality, we will assume $t_0 = 0$ in the following.

Step-1 Compute the new position of the moving boundary by:

$$\frac{\eta^{n+1} - 2\eta^n + \eta^{n-1}}{\Delta t^2} + a \cdot \frac{\eta^{n+1} - \eta^{n-1}}{\Delta t} + a^2 \eta^{n+1} = \gamma(P^n - P_{ext}) \quad (4)$$

Step-2 Deduce boundary velocity for the fluid and the mesh:

$$u_{|\Gamma^{n+1}}^{n+1} = C_{|\Gamma^n} = \frac{\eta^{n+1} - \eta^n}{\Delta t} \quad (5)$$

Step-3 compute the mesh velocity C by:

$$\begin{cases} \Delta C = 0 \\ C_{|\Gamma^n} = u_{|\Gamma^{n+1}}^{n+1} \end{cases} \quad (6)$$

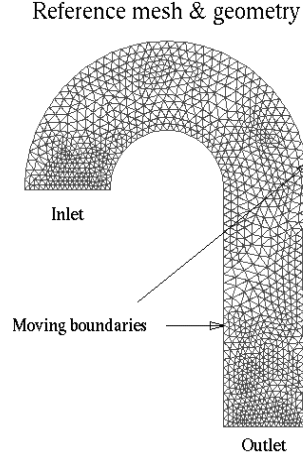
Step-4 Extend the mesh:

$$x^{n+1} = x^n + \Delta t.C \quad (7)$$

Step-5 Convection of the fluid by a method based on the analysis of the characteristics. Gives \tilde{u}^{n+1} , solution at time $(n+1).\Delta t$ of:

$$\int_{n\Delta t}^{(n+1)\Delta t} \frac{\partial u}{\partial t} + (u - C). \nabla u = 0 \quad (8)$$

Figure 1: Simplified aortic arch



Step-6 Stokes step. Compute u^{n+1} and P^{n+1} by:

$$\begin{cases} \frac{u^{n+1} - \tilde{u}^{n+1}}{\Delta t} - \nu \Delta u^{n+1} + \nabla P^{n+1} = 0 \\ \nabla \cdot u^{n+1} = 0 \\ u|_{\Gamma^{n+1}} = \eta^{n+1} - \eta^n \end{cases} \quad (9)$$

Remark The term $a. \frac{\eta^{n+1} - \eta^{n-1}}{\Delta t}$ in equation (4) is given in parenthesis because it was only added for numerical convenience to stabilize the algorithm.

4.4 Preliminary Results

As first step we executed the code for a rigid configuration (no moving boundaries). This configuration allowed us to test the flexibility of the fluid simulation code N3S (by Simulog) for quite irregular pulsed inlet velocity boundary conditions. These conditions are based on experimental values obtained on an artificial simulator of the cardiovascular system (data courtesy of Sorin Biomedica). We noticed that the fluid solution well behaved even after inversion of the flow. This flow inversion induces an entering velocity at the “outlet” Neumann boundary. The reflux in the aortic artery at the beginning of the diastole, which lasts for its entire duration in case of an artificial or injured aortic valve, has too strong influence on the characteristics of the flow to be artificially neglected (by smoothing or artificially increasing the inlet flow), even if it corresponds to a small fraction of the total loading. As a consequence of the good behavior obtained, we introduced a fluid-structure coupling by using the first of the two pressure laws previously indicated, (relation (1)) on the wall. After very encouraging initial results, with large time steps and coarse grids, we could not proceed

further because of very strong instability of the solution. In contrast with usual stability results, this instability grows as the time step (taken constant during the whole computation) decreases. By observing how instabilities developed we were led to think that they were due to a strong stiffness of the wall pressure law. A pressure perturbation induces an almost instantaneous displacement of the wall, causing strong velocity variations which produce an amplified big jump of pressure. So, we introduced the second wall-pressure law (2) for the fluid structure coupling. To get rid of the natural oscillatory modes of the moving boundary, we added a dissipation term of the form $C.\eta'$ in the equation. The coefficient was chosen in a way to get a double real negative eigenvalue for the associated homogeneous linear differential equations. We also made implicit the finite difference scheme describing the temporal progression of the walls. This new procedure was tested. It provides a system with a better stability than before but not yet sufficient. What is worse is that the pathological behavior of the numerical solution with the decrease of the time step is preserved. This means that the principal source of instability is still to be found. Nevertheless, this small gain allowed us to detect, just before or at the beginning of the spreading of the instability, a strange behavior of the flow at the Neumann outlet. A more elaborated study on the consequences of this type of boundary condition maybe could give us a criterion to modify in a more correct, if not the less harmful, way.

5 Afterwards considerations

5.1 A priori estimates on the continuous equations

We want to give an a priori estimate which could allow us a better understanding of the problem. We consider then a simplified problem where dissipative terms are neglected.

Let Ω be a domain whose boundary Γ is composed of three parts:

1. Γ_1 is supposed to be an inlet, with Dirichlet boundary condition on the velocity field;
2. Γ_2 is supposed to be an outlet, with a priori Neumann type boundary condition on the velocity field;
3. Γ_3 is the interface with the elastic wall. Pressure and velocity are the same on both sides of the interface.

The coupled system is written as:

$$u' + (u.\nabla)u + \nabla P = 0 \text{ in } \Omega \quad (10)$$

$$\eta'' + \eta = P \text{ on } \Gamma_3 \quad (11)$$

$$u|_{\Gamma_3}.n = \eta' \quad (12)$$

Multiplying (10) by u and integrating over Ω , we get

$$\frac{1}{2}\partial_t|u|_{L^2(\Omega)}^2 + \frac{1}{2}\int_{\Gamma_1+\Gamma_2}|u|^2u.n + \int_{\Gamma}Pu.n = 0. \quad (13)$$

Multiplying (11) by η' and integrating over Γ_3 , we get

$$\frac{1}{2}\partial_t|\eta'|_{L^2(\Gamma_3)}^2 + \frac{1}{2}\partial_t|\eta|_{L^2(\Gamma_3)}^2 = \int_{\Gamma_3}P\eta'. \quad (14)$$

Summing these two equations, we have

$$\frac{1}{2}\partial_t(|u|_{L^2(\Omega)}^2 + |\eta'|_{L^2(\Gamma_3)}^2 + |\eta|_{L^2(\Gamma_3)}^2) = -\int_{\Gamma_1+\Gamma_2}\left(\frac{1}{2}|u|^2 + P\right)u.n \quad (15)$$

From this estimate, we can see that the instabilities can either be caused by high flow in outlet or by high pressure values. In fact, numerical simulations can give both these numerical phenomena.

If we keep in mind our specific problem, with its own orders of magnitude, the simplified coupled system is better described modifying equation (11) by:

$$\epsilon\eta'' + \eta = P \text{ on } \Gamma_3, \quad (16)$$

where $\epsilon \approx \rho_w h$, cf. equation (2), is a small parameter with order of magnitude 10^{-6} .

In this case, we get the a priori estimate:

$$\frac{1}{2}\partial_t(|u|_{L^2(\Omega)}^2 + \epsilon|\eta'|_{L^2(\Gamma_3)}^2 + |\eta|_{L^2(\Gamma_3)}^2) = -\int_{\Gamma_1+\Gamma_2}\left(\frac{1}{2}|u|^2 + P\right)u.n. \quad (17)$$

From this estimate, it is now clear that η' is not strictly controlled by the kinetic and pressure energy put in inlet and outlet.

Another a priori estimate that gives a control over the velocity of the moving wall is obtained multiplying the structural equation by ϵ^{-1} as it follows:

$$\begin{aligned} \frac{1}{2}\partial_t(|u|_{L^2(\Omega)}^2 + |\eta'|_{L^2(\Gamma_3)}^2 + \epsilon^{-1}|\eta|_{L^2(\Gamma_3)}^2) &= -\int_{\Gamma_1+\Gamma_2}\left(\frac{1}{2}|u|^2 + P\right)u.n \\ &+ (\epsilon^{-1} - 1)\int_{\Gamma_3}Pu.n. \end{aligned} \quad (18)$$

This means that to have a reasonable control over η' you must perfectly control the pressure on Γ_3 . Unfortunately, this is not what happened in our first attempts. Moreover, the simulations we were able to run for for a reasonable number of time steps were obtained using an added mass, which consists in taking a much bigger h (1cm instead of 1mm). In terms of these a priori estimates, it means that we took ϵ ten times as big, reducing in the same way the sensibility of the wall to the pressure.

5.2 A pathological situation

Let Ω be a disk and its boundary Γ an elastic wall. We begin with an equilibrium state in which internal and external pressures are equal and the fluid is still. At $t = t_0$, we force the external pressure to decrease uniformly on Γ .

How should the system react?

- 1 The internal pressure should instantaneously uniformly decrease according to the external pressure.
- 2 The fluid should stay still.

Now let's consider how will our algorithm react to such a situation.

- 1 at Step 1 and 2, the boundary Γ gets lightly uniformly extended and a positive normal velocity is set on it.
- 2 Steps 3 to 5, everything goes well.
- 3 At step 6, the projection step, we are required to solve

$$\begin{cases} \Delta P = \nabla \cdot \tilde{u}^{n+1} \text{ on } \Omega^{n+1} \\ \nabla P \cdot n = 0 \text{ on } \Gamma^{n+1} \end{cases} \quad (19)$$

which has no solution because of the compatibility condition that we get integrating equation (19) over Ω^{n+1} :

$$\int_{\Gamma^{n+1}} \nabla P \cdot n = \int_{\Gamma^{n+1}} \tilde{u}^{n+1}. \quad (20)$$

So, in this situation, the algorithm fails instantaneously. Now, let us consider the same domain with a tiny hole on the elastic boundary. This hole is modeled with a Neumann boundary condition on the velocity field. In the situation given above the system should have the same reaction: it stays still. Following the algorithm, we can proceed until step 6. Now there is a solution to the pressure correction which consists in giving a very high value to the entering flow at the level of the hole to preserve the conservation of the mass. The mean velocity value on this part of the boundary is proportional to the velocity on the elastic wall and to the ratio of the areas of the two boundaries. The higher is the ratio, the less reliable is the algorithm behavior.

5.3 Time scale inconsistency

The pathological case just described allows us to understand why we have a possibility of strong instabilities of the scheme. It doesn't explain why we managed to get seemingly reasonable results for large Δt , of order of a few $10^{-3}s$.

When we want to understand the behavior of the moving wall, a useful quantity is the characteristic time given by the dynamic equation of the structure. In our case it is given by $T_w = \frac{1}{a}$ where a is the quantity in equation (4). When

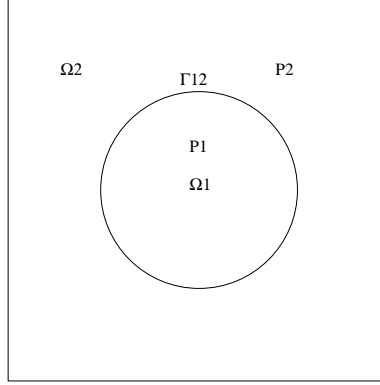


Figure 2: Pathological case. For a numerical algorithm, the pressure $P1$ should know any uniform change of $P2$ without movement of the elastic boundary Γ_{12} when the flow is still.

we let free the wall after an initial static deformation η_0 , the time dependent deformation is given by:

$$\eta = \eta_0 \cdot e^{-\frac{t-t_0}{T_w}} \quad (21)$$

when we keep the friction term, and by:

$$\eta = \eta_0 \cdot \cos\left(\frac{t-t_0}{T_w}\right) \quad (22)$$

when we don't consider it.

From expression (2) we get:

$$T_w = \sqrt{\frac{\rho_w \cdot (1 - \nu^2) \cdot R^2}{E}} \quad (23)$$

with the radius taken constant at $15mm$,
the wall density at $\rho_w = 1.1 \cdot 10^{-6} kg.mm^{-3}$,
the Young coefficient at $E = 3 \cdot 10^2 kg.mm^{-1}.s^{-2}$
and the Poisson coefficient at $\sigma = 0.5$, relation (23) gives:

$$T_w \approx 0.8 \cdot 10^{-3} s. \quad (24)$$

In fact, when we perform a simulation with $\Delta t = 5 \cdot 10^{-3}$, we obtain a solution seemingly reasonable. Taking $\Delta t = 2 \cdot 10^{-3}$, the solution begins to degenerate at the Neumann outlet. For $\Delta t = 10^{-3}$, the solution is highly degenerated at the outlet and begins to pollute the flow upstream. For smaller Δt we get fast explosion.

So, we manage to get a solution only when we don't solve correctly the interaction time scale and, because of the implicit treatment of the structure equation, we are artificially increasing the diffusive properties of the scheme.

5.4 Pressure correction default

The analysis of the scheme will now be extended, with the aim of finding an improvement. First, let's get a better insight of the treatment of the pressure considering the following example.

Let Ω be a $2D$ rectangular domain with periodicity condition on the top and bottom velocities, time dependent Dirichlet velocity condition on left-side (inlet) and Neumann velocity condition on the right (outlet) (see figure 5.4). The equations of the continuous are given by:

$$\begin{cases} u' + (u \cdot \nabla)u - \mu \cdot \Delta u + \nabla P = 0 & \text{in } \Omega \\ u|_{\Gamma_1} = g(t) & \text{with } g(t) \wedge n = 0 \\ u|_{\Gamma_{31}} = u|_{\Gamma_{32}} \\ \nabla u \cdot n = 0 & \text{on } \Gamma_3 \\ P|_{\Gamma_2} = P_{out}(t). \end{cases} \quad (25)$$

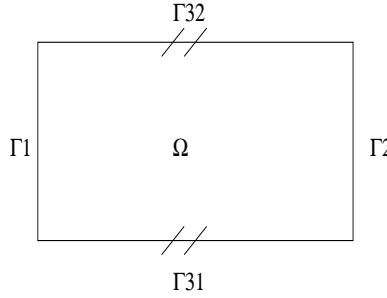


Figure 3: Domain periodical orthogonally at the inlet flow. For such a domain and an horizontal flow, uniform in space, we know an explicit solution. The numerical scheme should approximate well this solution.

For this system, due to symmetry proprieties of symmetry, we can compute the exact solution which is:

$$\begin{cases} u = g(t) & \text{in } \Omega \\ P = P_{out}(t) + g'(t) \cdot (x|_{\Gamma_3} - x), \end{cases} \quad (26)$$

and moreover

$$u' + \nabla P = 0 \quad \text{in } \bar{\Omega}. \quad (27)$$

Let $g(0) = 0$ and $g'(0) = 0$. Now, let's follow the pressure evolution when computed with our algorithm and in particular its gradient in inlet. We have $\nabla P|_{\Gamma_1}^0 \cdot n = 0$. As we update the pressure with a correction verifying $\nabla Q|_{\Gamma_1} \cdot n = 0$, we have for all n : $\nabla P|_{\Gamma_1}^n \cdot n = 0$. Unfortunately this is completely untrue when u' is relatively high, as shown by equation (27).

6 Modified algorithm proposal

6.1 Determination of the reference pressure

Given the fluid movement, we know that the pressure field is known up to a constant. We will now propose a method to calculate this constant in a quite general and simple way. The idea is the following:

when ∇P is derived from the zero divergence equation for the velocity field $\nabla \cdot u = 0$, the reference pressure P_{ref} will be derived by the zero divergence equation for the acceleration field $\nabla \cdot u' = 0$, as we will now explain.

Given in integral form on the boundary, we get:

$$\int_{\Gamma} u' \cdot n = 0. \quad (28)$$

Let's suppose for a moment that $|\Gamma_3| = 0$, i.e. there is no Neumann boundary condition. So:

$$\int_{\Gamma} u' \cdot n = \int_{\Gamma_1} u' \cdot n + \int_{\Gamma_2} u' \cdot n. \quad (29)$$

We have $u'_{|\Gamma_1} = g'(t)$ prescribed and $u'_{|\Gamma_2} \cdot n = \eta''$ where η is the displacement of the wall.

Usually, the structural law is of the form:

$$\eta'' = F(\eta, \eta', \partial_x, \dots, P_0) + \gamma P \quad (30)$$

where all the arguments of F are explicitly known at computational time. So, writing the pressure P as $P = \tilde{P} + C$ where \tilde{P} is a pressure guess and C a spatially constant correction, we get:

$$\int_{\Gamma_1} g'(t) \cdot n + \int_{\Gamma_2} (F + \gamma \tilde{P}) + \gamma \cdot |\Gamma_2| \cdot C = 0 \quad (31)$$

or

$$\int_{\Gamma_1} g'(t) \cdot n + \int_{\Gamma_2} \tilde{\eta}'' + \gamma \cdot |\Gamma_2| \cdot C = 0 \quad (32)$$

where $\tilde{\eta}''$ is the acceleration guess corresponding to \tilde{P} . Isolating C , we have:

$$C = - \frac{\int_{\Gamma_1} g'(t) \cdot n + \int_{\Gamma_2} \tilde{\eta}''}{\gamma \cdot |\Gamma_2|} \quad (33)$$

and the pressure is fixed by a correction to the initial guess.

Let's consider the case when there is a Neumann boundary condition on the flow. A Neumann outlet is usually a convenient way to artificially bound a domain which is fundamentally either unbounded or with boundaries so far away to make impossible an analysis on the whole physical domain. The location of the artificial Neumann boundary is rather arbitrary, as long as it can be reasonably felt that the flow approximately satisfies the Neumann condition. So, we shall also turn to valuate $\int_{\Gamma_3} u' \cdot n$ in an approximated manner.

For a very small time interval, we can imagine that Γ_3 is a physical “wall” with a given velocity and a part of the boundary of another system out of the domain. We just have to evaluate in term of boundary acceleration what is the answer of this system to a given surface pressure.

For example (see figure 6.1), considering the outside boundary of the simplified aortic arch, we can think of the external system as a tube of length L in which the work of the pressure compensate the kinetic energy variation and the friction dissipation. That gives:

$$\int_{\Gamma_3} u'.n = \int_{\Gamma_3} [L^{-1}.P - k.u.n] \quad (34)$$

$$= \int_{\Gamma_3} [L^{-1}.\tilde{P} - k.u.n] + \frac{|\Gamma_3|.C}{L}. \quad (35)$$

The correction to the guess pressure is then given by:

$$C = -\frac{\int_{\Gamma_1} g'(t).n + \int_{\Gamma_2} \tilde{\eta}'' + \int_{\Gamma_3} [L^{-1}.\tilde{P} - k.u.n]}{\gamma.|\Gamma_2| + |\Gamma_3|.L^{-1}}. \quad (36)$$

6.2 Modified algorithm

We are now capable to propose a new version of the entire resolution algorithm for ALE-based fluid structure interaction resolving at least the difficulties risen in the previous part.

The ALE formulation requires the computation of a domain velocity C . Wanting to be coherent with the boundary conditions, we choose to solve a dynamic system for the velocity C of the domain

. The system of equations to solve for the continuous problem is:

$$\left\{ \begin{array}{l} u' + (u - c).\nabla u + \nabla P - \mu\Delta u = 0 \\ \eta'' + F(\eta, \eta', \partial_x, \dots, P_0) = \gamma P \\ c' - \mu_c \Delta c = 0 \\ c_{\Gamma_{1+3}}.n = 0 \\ c_{\Gamma_2} = u_{\Gamma_2} \\ u_{\Gamma_1} = g(t, x) \\ u_{\Gamma_2}.n = \eta' \\ u_{\Gamma_2} \wedge n = 0 \\ \bar{p} = h(u') \\ \partial_n u_{\Gamma_3}.n = 0. \end{array} \right. \quad (37)$$

The ALE formulation require the computation of a grid velocity C .

We write \bar{p} for any chosen quantity that fixes the indetermination of the pressure. We suppose all the quantities known at iteration n . We denote by a $\tilde{}$ (tilde) an intermediary solution and the exponent refers to the mesh upgrade.

Step1 Fix the pressure indetermination. Gives \tilde{P}^n .

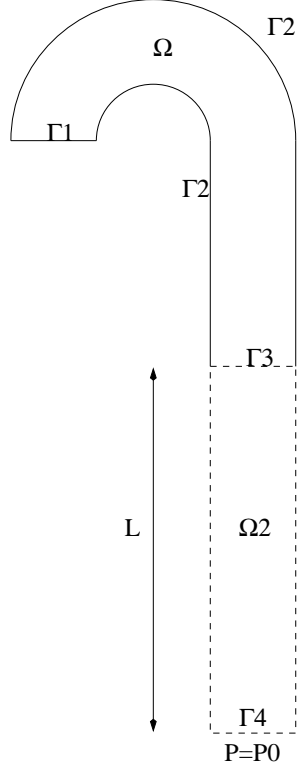


Figure 4: We evaluate the pressure on Γ_3 by fictively adding a new domain Ω_2 where the flow and pressure patterns are given by simple integral laws.

Step2 Compute η^{n+1} by using the structural software.

Step3 Compute $u_{\Gamma_2}^{n+1}$ by the formula:

$$u_{\Gamma_2}^{n+1} = 2 \cdot \frac{\eta^{n+1} - \eta^n}{\Delta t} - u_{\Gamma_2}^n. \quad (38)$$

Step4 Compute the velocity c of the mesh at time step $n + 1$.

$$\begin{cases} \tilde{c}^n - \Delta t \cdot \mu_C \cdot \Delta \tilde{c}^n = c^n \\ \tilde{c}_{\Gamma_2}^n = u_{\Gamma_2}^{n+1} \\ \tilde{c}_{\Gamma_1 + \Gamma_3}^n = 0. \end{cases} \quad (39)$$

Gives \tilde{c}^n

Step5 (Convection on the old mesh)

By any adapted method (characteristics), solve

$$\begin{cases} \tilde{u}^n = u^n + \Delta t \cdot [(u - c^n) \cdot \nabla u + \nabla P] \\ \tilde{u}_{\Gamma_1}^n \cdot n = g^n \cdot n \\ \tilde{u}_{\Gamma_2}^n \cdot n = u_{\Gamma_2}^n \cdot n. \end{cases} \quad (40)$$

Gives \tilde{u}^n .

Step6 Compute the new mesh by using the mesh velocity and position field.

$$X^{n+1} = X^n + \frac{\Delta t}{2} \cdot (\tilde{C}^n + C^n). \quad (41)$$

Gives X^{n+1} and C^{n+1} .

Gives also \tilde{u}^{n+1} and \tilde{P}^{n+1} .

Step7 (Diffusion step on the new mesh) Solve:

$$\begin{cases} \tilde{u}^{n+1} - \Delta t \cdot \mu \Delta \tilde{u}^{n+1} = \tilde{u}^{n+1} \\ \tilde{u}_{\Gamma_1}^{n+1} = g^n \\ \tilde{u}_{\Gamma_2}^{n+1} = (\eta^n, 0) \\ \partial_n \tilde{u}_{\Gamma_3}^{n+1} \cdot n = 0. \end{cases} \quad (42)$$

Gives \tilde{u}^{n+1} .

Step8 (Projection step) Compute Q , a pressure increment, solving:

$$\begin{cases} -\Delta Q = \nabla \cdot \tilde{u}^{n+1} \\ \partial_n Q_{\Gamma_1} \cdot n = (g^{n+1} - g^n) \cdot n \\ \partial_n Q_{\Gamma_2} \cdot n = (u^{n+1} - u^n)_{\Gamma_2} \cdot n \\ Q_{\Gamma_3} = 0. \end{cases} \quad (43)$$

Step9 Correct to get the velocity and pressure at time step $n + 1$.

$$u^{n+1} = \tilde{u}^{n+1} + \nabla Q \quad (44)$$

$$P^{n+1} = \tilde{P}^{n+1} + Q. \quad (45)$$

Obviously, numerous variations can be discussed, such as transferring the pressure on the left hand side from the convection to the diffusion step. We can also fix the tangential velocity at $g^{n+1} \wedge n$ at the diffusion step. Indeed these variations don't modify the characteristics that we required for the scheme.

7 Conclusion

The first part of this work has been done during the Cemracs96 intensive research center in Marseille.

It allowed both the authors to get more familiar to the quite wide range of knowledge needed to tackle the subject, going from numerical analysis and scientific computing to biomechanics.

We were wondering why we could not find in the literature other people doing full coupled Navier-Stokes and structural simulation of the aorta. The most complete similar work is done by Perktold&alt. (see ref.) in the context of

the carotid bifurcation. Although it was a 3D simulation, there is no use of any kind of ALE technique so we can't expect results asymptotically too accurate.

Since that not being able to give reliable results that take in consideration the physical time scales of the problem could be considered as a failure, we turned in the second part to a deeper analysis of the computational scheme.

We showed that our calculus algorithm, which is what we can find of best in this area, cannot solve accurately this kind of situation, being intrinsically unstable except at the cost of denaturing the physics underlying.

We have given a simple benchmark case that any proposed algorithm should be easily able to correctly solve. This could be interpreted as a minimum consistency check.

We showed that the treatment of the pressure is of critical importance and approximation errors must be carefully analyses.

We hope that the analysis developed here can give to people new to this kind of studies hints on what to do and advises on errors not to fall in.

A new algorithm verifying the conditions stated in the second part of this work is now under development.

8 Acknowledgments

The authors thank Prof. Yvon Maday who organized the Cemracs96 where this study was initiated. We are grateful to Simulog for providing free access of the software N3S, SIMAIL and ENSIGHT during the Cemracs period.

Vincent Moreau was supported under the Human Training and Mobility program Contract CHRV-CT93-0420 and is indebted to the Sardinia Autonomous Region who permitted him to carry out his research at the CRS4.

9 References

ANLIKER M., ROCKWELL R.L. and ODGEN E. (1971)
Non linear analysis of flow pulses and shock waves in arteries I & II
Z.Angew Math. Phys. 22, 217-46 & 563-81

ATABEK H.B., LING S.C. (1973)
Non linear analysis of pulsatile flow in arteries
J. Fluid Mech. 55, pp 493-511.

ATABEK H.B. (1980)
Blood flow and pulse propagation in arteries. Basic hemodynamics and its role in disease Processes
University Park Press, Baltimore.

BELARDINELLI E., CAVALCANTI S. (1992)
Theoretical analysis of pressure pulse propagation in arterial vessels. J. Biomechanics Vol. 25, 1337-1349.

BLANCO A.(1995)
Quelques aspects de l'écoulement d'un fluide visqueux autour d'une bulle déformable : une analyse par simulation directe
Thèse de L'institut national Polytechnique de Toulouse

BUTHAUD H. (1976)
Analyse non linéaire de l'écoulement sanguin dans un modèle de l'aorte.
Ph.D.Thesis, Université de Poitiers.

CARO C.G. , FITZ-GERALD J.M. and SCHROTER R.C. (1971)
Atheroma and arterial wall shear: observation, correlation and proposal of shear dependent mass transfer mechanism for atherogenesis. Proc.R.Soc.Lond, 177, 109-159.

CAVALCANTI (1995)
Hemodynamics of an artery with mild stenosis.
J.Biomechanics Vol. 28 n4 pp 387-399.

DOUFOULKAR Z., OUAZZINI M.T., KHALID-NACIRI J.and ZAGZOULE M. (1995) Modélisation de l'écoulement d'un fluide visco-élastique en conduite souple : Application à l'aorte.
Journal of Physics III.

DUTTA A., TARBELL J.M. (1989)
Numerical simulation of sinusoidal flow in a straight elastic tube: effects of phase angle.
Biorheology Vol 26 , pp 1-22.

DUTTA A., WANG D.M., TARBELL J.M. (1992)
Numerical analysis of flow in an elastic artery model
J. Biomechanical Engineering Vol 114.

FLAUD P.(1979) Influence des propriétés rhéologiques non linéaires sur la dynamique des écoulements dans un tuyau déformable.
Thèse d'état. Université PARIS VII.

FUNG Y.C., FRONEK K., PATITUCCI P. (1979)
Pseudo-elasticity of arteries and the choice of its mathematical expression American Journal of Phys.

KHALID-NACIRI J. (1988)
Contribution à la modélisation d'écoulements instationnaires en conduites déformables.

Thèse d'Etat Université Paul Sabatier, Toulouse.

KLANCHARD M., TARBELL J.M., WANG D.M.(1990)

In vitro study of the influence of radial wall motion on wall shear stress of the aorta.

Circulation research Vol 66, No 6 , pp 1624-1635.

KUFAHL R.H. and CLARK M.E. (1985)

A circle of Willis simulation using distensible and pulsatile flow.

J.Biomech.Eng 107,pp112-122.

LAGRÉE P.-Y. et ROSSI M.

Étude de l'écoulement du sang dans les artères : effets nonlinéaires et dissipatifs.

C.R. Acad. Paris, t.332, Série II b, p. 401-408, 1996

LAMBOSSY P. (1952)

Oscillations forcées d'un liquide incompressible et visqueux dans un tube horizontal calcul de la force de frottement.

Helvetica Physica Acta 25, 371-381.

LAURENS P.(1994)

Modélisation et simulation numérique de l'écoulement coronarien : effets de la contraction cardiaque.

Ph.D. Thesis. Université Paul Sabatier Toulouse.

LOU Z., YANG W.J., STEIN P.D. (1993)

Errors in the estimation of the arterial wall shear rates that result from curve fitting of velocity profiles.

J. Biomechanics Vol 26 pp 383-390.

Ma X., LEE G.C. and WU S.G.(1992)

Nonlinear pulsatile Waves in arteries.

J.Biomechanics 27,277-287.

MEDERIC P., GAUDU R., MAUSS J. and ZAGZOULE M. (1991)

Modélisation unidimensionnelle des écoulements instationnaires en conduites souples : application au cathétérisme cardiaque.

Innov.Tech.Biol.Med. 12, 233-243.

MEISTER J.J. (1983)

Mesure par échographie doppler et modélisation théorique de l'effet des troubles cardiaques sur la pression et le débit artériel.

Ph.D. Thesis, E.P.F. Lausanne,Switzerland.

OLUFSEN M., OTTESEN J. (1995)

A fluid dynamical model of the aorta with bifurcations

Rodskilde Universitetscenter technical report, TESK NR296

- PATEL D. J., VAISHNAV R.N. (1980)
Basic Hemodynamics and its role in disease processes
University Park Press, Baltimore.
- PEDLEY T.J. (1980)
The fluid mechanics of large blood vessels.
Cambridge University Press.
- PERKTOLD K., THURNER E., KENNER T. (1994)
Flow and stress characteristics in rigid wall and compliant carotid artery bifurcation models.
Med. Biol. Eng Comput., Vol 32, pp 19-26.
- PERKTOLD K., RAPPITSCH G. (1995)
Computer simulation of local blood flow and vessel mechanics in a compliant carotid artery bifurcation model
J. Biomechanics Vol 28, No 7, pp 845-856
- PORENTA G., YOUNG D.F. and ROGGET T.R.(1989)
A finite element method of blood flow in arteries including taper branches and obstructions.
J.Biomech.Engng. 113, 464-475.
- REUDERINK, P. (1991)
Analysis of the flow in 3D distensible model of the carotid artery bifurcation.
Ph.D. Thesis, Eindhoven, Netherland.
- STERGIOPOULOS N., TARDY Y., MEISTER J.J. (1992)
A method for the non invasive estimation of the arterial compliance
Bed Vol22, Advances in Bioengineering, ASME.
- TARDY Y. (1992)
Non-invasive characterization of the mechanical properties of arteries
These de l'ecole polytechnique de Lausanne.
- YAMA, J.R., MEDERIC P. and ZAGZOULE M. (1995)
Etude comparative des differentes approximations de la contrainte de cisaillement à la paroi.
submitted to J.Phys III.
- WANG D.M., TARBELL J.M.(1991)
Non linear-analysis of flow in an elastic tube (artery): steady streaming effects.
- WOMERSLEY J.R.(1957a)
Oscillatory flow in arteries: the constrained elastic tube as a model of arterial

flow and pulse transmission.
Phys. Med. Biol Vol 2, pp 178-187.

WOMERSLEY J.R.(1957b)
An elastic tube theory of pulse transmission and oscillatory flow in mammalian arteries.
WADC Tech.Rep 56-614

ZAGZOULE, M. (1987)
Modélisation mathématique de la circulation sanguine cérébrale : aspects instationnaires et non-newtoniens
Thèse Doctorat d'Etat. Université Paul Sabatier, Toulouse.